



Dalton
Transactions

Atomic-precision engineering of metal nanoclusters

| | |
|-------------------------------|---|
| Journal: | <i>Dalton Transactions</i> |
| Manuscript ID | DT-FRO-05-2020-001853.R1 |
| Article Type: | Frontier |
| Date Submitted by the Author: | 19-Jun-2020 |
| Complete List of Authors: | Du, Xiangsha; Carnegie Mellon University, Chemistry Jin, Rongchao; Carnegie Mellon University, Chemistry |
| | |

SCHOLARONE™
Manuscripts

Atomic-precision engineering of metal nanoclusters

Xiangsha Du and Rongchao Jin*

Received 00th January 20xx,
Accepted 00th January 20xx

DOI: 10.1039/x0xx00000x

Ultrasmall metal nanoparticles (below 2.2 nm core diameter) start to show discrete electronic energy levels due to strong quantum confinement effects and thus behave much like molecules. The size and structure dependent quantization induces a plethora of new phenomena, including the multi-band optical absorption, enhanced luminescence, single-electron magnetism, and catalytic reactivity. Exploration of such new properties is largely built on the success in unveiling the crystallographic structures of atomically precise nanoclusters (typically protected by ligands, formulated as $M_nL_m^q$, where, M = metal, L = Ligand, q = charge). Correlation between the atomic structures of nanoclusters and their properties has further enabled atomic-precision engineering toward materials design. In this Frontier article, we illustrate several aspects of precise engineering of gold nanoclusters, such as the single-atom size augmenting, single-atom dislodging and doping, precise surface modification, and single-electron control for magnetism. Such precise engineering involves the nanocluster's geometric structure, surface chemistry, and electronic properties, and future endeavors will lead to new materials design rules for structure-function correlations and largely boost applications of metal nanoclusters in optics, catalysis, magnetism, and other fields. Following the illustrations of atomic-precision engineering, we have also put forth some perspectives. We hope this Frontier article to stimulate research interest in atomic-level engineering of nanoclusters.

Introduction

Nanoscience is largely built on the breakthroughs in the synthesis of high-quality nanoparticles. Recently, nanoscience has moved on to the atomic-precision stage owing to the successful development of atomically precise nanochemistry.¹ New methodologies for the controlled synthesis of atomically precise metal nanoclusters have been well developed.¹⁻⁴ A recent focus is to investigate the new physicochemical properties of metal nanocluster materials.^{5,6} The discrete electronic structure of nanoclusters induces a plethora of new physical and chemical properties.⁷⁻⁹ For example, the quantum confinement effects in nanoclusters has recently been mapped out to have multiples stages in the size evolution¹⁰ and also a strong dependence on the crystal structures.⁷ The successfully determined structures of nanoclusters provide atomic-level understanding of the new physicochemical properties.¹⁻⁵ Built on such successes, it has now been possible to start precise engineering on the nanocluster structure and properties.⁵

Generally, the atomically precise nanoclusters can be formulated as $M_nL_m^q$ (where, M = metal, L = ligand, q = charge). The atomic arrangements of metal kernel and surface-protecting motifs, as well as the overall charge, give rise to rich families of nanoclusters.^{11, 12, 13}

The number of atoms, the type of atoms, geometric packing and charge state are all important parameters for the nanoclusters, thus, one can expect that subtle changes to those variables could induce intriguing properties of this new class of nanomaterials. Investigations on the atomic level engineering of nanoclusters have shown great progress.^{1-4, 14}

In this Frontier article, we illustrate the atomic level engineering in metal nanoclusters, (i) the metal component engineering for optical properties and catalytic reactivity, (ii) surface-protecting ligand engineering for catalysis, and (iii) the charge state engineering for magnetism. The metal component engineering is quite rich, including the single-atom increment, single-atom shuttling in and out, doping single foreign atom, and molecular "surgery" on nanoclusters. Representative examples are highlighted for each category. We hope that this Frontier article could stimulate future interest and new strategies on atomic-level engineering of nanocluster materials.

Metal component engineering

Single-atom increment in Au_{23} , Au_{24} and Au_{25}

Taking gold nanoclusters as an example, their properties exhibit high sensitivity to the size (i.e. the number of Au atoms). By adding or removing a single gold atom, significant changes may be induced in the structure and properties; for example, Au_{23} , Au_{24} and Au_{25} as a trio of consecutive-size nanoclusters¹⁵⁻¹⁷ (Figure 1a-c) show dramatically different kernel and surface structures and, accordingly, very different catalytic activity in the reaction of 4-nitrophenol (4-NP) reduction to aminophenol.¹⁸ Among the trio, $[Au_{23}(SR)_{16}]^-$ exhibits the highest kinetic rate constant of 0.037 s^{-1} , which is much higher than the rate constants of $Au_{24}(SR)_{20}$ (0.009 s^{-1}) and $[Au_{25}(SR)_{18}]^-$ (0.024 s^{-1}) (Figure 1d-g). The $[Au_{23}(SR)_{16}]^-$ nanocluster contains an Au_{13} cuboctahedron kernel as opposed to the bi-tetrahedral Au_8 kernel in $Au_{24}(SR)_{20}$ and the icosahedral Au_{13} kernel in $[Au_{25}(SR)_{18}]^-$. The surface protecting staple motifs also vary from each other.¹⁵⁻¹⁷ Concomitant with the distinctively different geometric structures, the electronic

Department of Chemistry, Carnegie Mellon University, Pittsburgh, PA 15213, USA.
Email: rongchao@andrew.cmu.edu.

properties also play major roles in affecting the catalytic performance. The numbers of free valence electrons of the $[\text{Au}_{23}(\text{SR})_{16}]^-$, $\text{Au}_{24}(\text{SR})_{20}$, and $[\text{Au}_{25}(\text{SR})_{18}]^-$ nanoclusters are 8, 4, and 8, respectively, and thus each gold atom bears 0.35, 0.17, and 0.32 electronic density on average. Of note, the number of free electrons, n^* , is simply counted by $n^* = nV_A - m - q$ for $[\text{M}_n(\text{SR})_m]^\pm$, where V_A is the valence of the metal atom, e.g. gold is monovalent due to $6s^1$, whereas Cd or Hg is divalent due to ns^2 , and Pd or Pt is typically counted as zero due to s to d electron transfer to form $(n-1)d^{10}ns^0$. As the higher electronic density facilitates the chemical reduction of 4-NP, it is reasonable that the catalytic activity follows an order of $[\text{Au}_{23}(\text{SR})_{16}]^- > [\text{Au}_{25}(\text{SR})_{18}]^- > \text{Au}_{24}(\text{SR})_{20}$. In this system, one can infer is that, instead of the nominal size (Au_{23} , Au_{24} and Au_{25} being very close in size), the different atom-packing modes and electronic structures dictate the catalytic difference. The available structures of nanoclusters also permit other deep investigations such as the electron transfer rate, energy barrier, steric barrier from the ligand shell, and catalytic intermediates in future work.

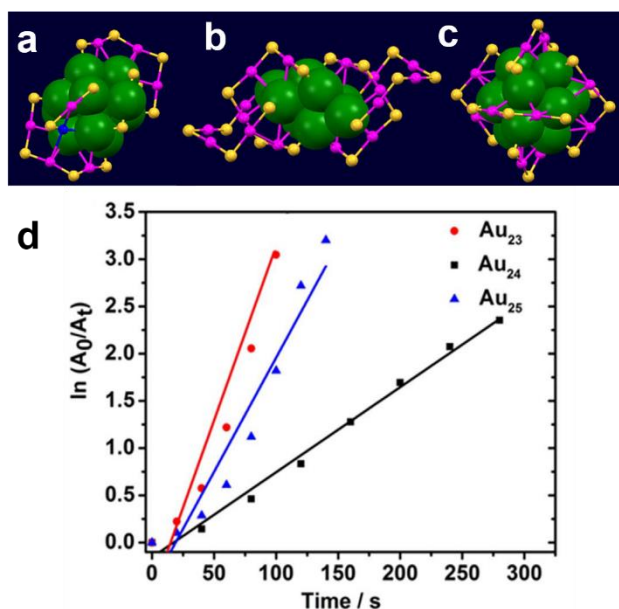


Figure 1. Crystal structures of $[\text{Au}_{23}(\text{SR})_{16}]^-$ (a), $\text{Au}_{24}(\text{SR})_{20}$ (b), and $[\text{Au}_{25}(\text{SR})_{18}]^-$ (c) with the R groups omitted for clarity; S, yellow; Au(motif), pink; Au(kernel), green/blue. UV-Vis spectroscopic monitoring of the catalytic reduction of 4-NP over Au_{23} (d), Au_{24} (e), and Au_{25} (f), and kinetic rate constants (the slopes) over the three nanoclusters (g). Panels (a) to (c): redrawn from refs. 15-17. Panel (d): adapted with permission from ref. 18, Copyright © 2016, Elsevier.

Single-atom shuttling in and out

Das et al. achieved a hollow $[\text{Au}_{24}(\text{PPh}_3)_{10}(\text{SC}_2\text{H}_4\text{Ph})_5\text{Cl}_2]^+$ nanocluster by dislodging a central gold atom out of the biicosahedral $[\text{Au}_{25}(\text{PPh}_3)_{10}(\text{SC}_2\text{H}_4\text{Ph})_5\text{Cl}_2]^{2+}$ with an excess of PPh_3 .¹⁹ Built on that, Wang et al. developed a capability of shuttling a single atom in and out of the nanocluster (Figure 2).²⁰ The Au_{24} has its central atom missing (i.e., corresponding to the shared vertex atom in the biicosahedral Au_{25}), which exerts a major influence on the optical properties. Wang et al.

demonstrated re-filling the central vacancy by single metal atom shuttling into the hollow Au_{24} structure through a reaction of Au_{24} with various metal salts, $\text{M}(\text{I})\text{Cl}$ ($\text{M} = \text{Au}, \text{Ag}, \text{Cu}$). It was found that such a reaction readily restores the 25-atom nanocluster, specifically, *single-atom* doped M_1Au_{24} , which was otherwise not attainable because Ag or Cu doping often leads to a distribution of dopants (more than one) as opposed to a single dopant atom. Single crystal X-ray diffraction analysis showed that Cu can occupy either the apex or waist positions of the rod-shaped nanocluster (Figure 2, right), while Ag was only found at the apex of the nanoparticle (Figure 2, left). The capability of single-atom shuttling in and out is the first demonstration, and the discovery of the dopant entering sites was also unprecedented.²⁰

Further experimental and theoretical investigations provided fundamental understanding of the process of shuttling a single atom in and out of the matrix. The driven force of single-atom dislodging or shuttling-out process lies in the free PPh_3 , and the surface $-\text{Cl}$ and $-\text{SR}$ ligands are responsible for the shuttling-in process of Ag and Cu atoms.²⁰ In addition to the shuttling mechanism study, a recent paper indicates that the internal vacancy of Au_{24} enhances the hydrogenation reaction of CO_2 .²¹ Taken together, shuttling a single atom in and out of the nanocluster system is an interesting strategy for atomic level engineering.

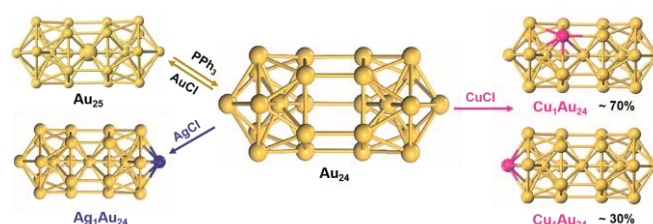


Figure 2. Single-atom shuttling in and out of the $\text{Au}_{24}/\text{Au}_{25}$; Au, yellow; Ag, blue; Cu, pink. The five SR, ten PPh_3 and two halide ligands are omitted for clarity. Adapted with permission from ref. 20. Copyright © 2017, Springer.

Single-atom doping

The properties of a metal can be effectively modified or enhanced by the addition of other metals, so-called alloying.²²⁻²⁶ The alloying strategy has played a significant role in metallurgy and applications since the Bronze Age about five thousand years ago.²⁷ Nowadays, atomic-level engineering through single-atom doping has become possible, which reveals unprecedented insights into the roles of metal composition and doping sites in tailoring the alloy nanocluster's properties.

For the $\text{Au}_{25}(\text{SR})_{18}$ nanocluster system, introducing single foreign atom M ($\text{M} = \text{Ag}/\text{Cu}/\text{Pt}/\text{Pd}/\text{Cd}/\text{Hg}$) into the parent Au_{25} cluster gives rise to $\text{M}_1\text{Au}_{24}(\text{SR})_{18}$ with the heteroatoms replacing Au atoms at different sites.²⁸⁻³⁹ Different from the central occupancy by Pt/Pd, Ag and Cu tend to go to the icosahedral shell sites. For the IIB elements, Cd is found on the icosahedral shell, while Hg replaces one Au atom from the ligand staple motif. Replacing the core Au atom with Pd or Pt

results in $[M_1Au_{24}(SR)_{18}]^0$ nanoclusters ($M = Pd, Pt$) with superatomic 6-electron configuration ($1S^21P^4$).³³

Similar to the Au_{25} system, a series of single-atom doped Ag_{25} clusters were later investigated.⁴⁰⁻⁴² The dopant atom in the $M_1Ag_{24}(SR)_{18}$ ($M = Au, Pt, Pd$) nanoclusters exclusively occupies the center of the icosahedron. This conforms to the rule of electronegativity.⁴³ Of note, the doping engineering in other cases includes single-Pt doping of Ag_{29} ^{44, 45} and single-Au doping of Cu_{25} ,⁴⁶ as well as centrally doped M_1Ag_{20} (where, $M = Pd, Pt, Au$)⁴⁷ and Au_1Ag_{33} ⁴⁸ nanoclusters.

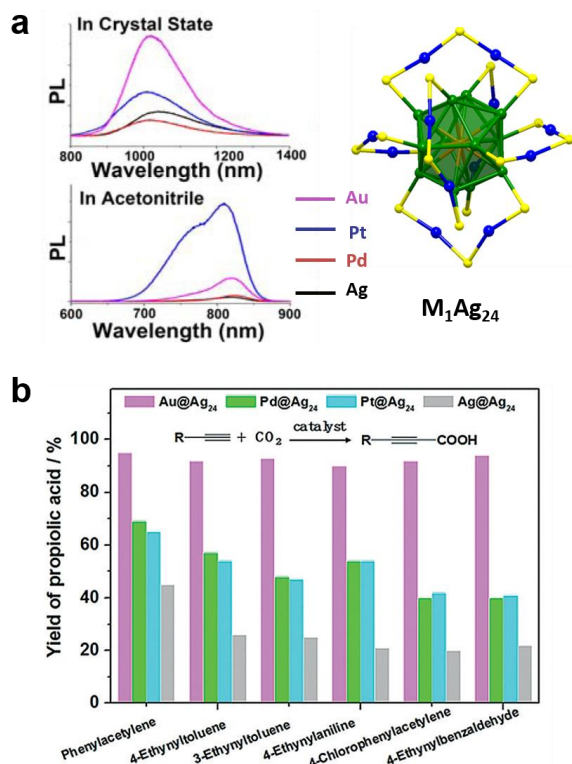


Figure 3. (a) Photoluminescence spectra and structural framework of $M_1Ag_{24}(SR)_{18}$ nanoclusters, color codes for the structure: S, yellow; Ag(kernel), green; Ag(surface), blue; central M ($M = Ag/Pd/Pt/Au$), orange; (b) The catalytic carboxylation of terminal alkyne with CO_2 over of $M_1Ag_{24}(SR)_{18}$ nanoclusters. Panel (a): adapted with permission from ref. 41; Copyright © 2017, American Chemical Society. Panel (b): adapted with permission from ref. 49; Copyright © 2018, Wiley.

Single-atom doping of nanoclusters also gives rise to enhancement of the properties, for example, the largely increased quantum yield in the doped $M_1Ag_{24}(SR)_{18}$ ($M = Au, Pt, Pd$) luminescence (Figure 3a).^{40, 41} In regards to the catalytic performance of $M_1Ag_{24}(SR)_{18}$ nanoclusters, Zhu and co-workers recently showed that foreign atom doping enhances the catalytic carboxylation of CO_2 with terminal alkyne (Figure 3b) and different foreign metal atoms offer different enhancement factors.⁴⁹

Both $M_1Au_{24}(SR)_{18}$ and $M_1Ag_{24}(SR)_{18}$ systems suggest that doping is a powerful means to tune the physical and chemical properties of the cluster, which has important implications for practical applications.

Molecular “surgery”

In contrast to the one-to-one metal exchange described above, site-specific molecular “surgery” on nanoclusters has also been demonstrated, which holds great promise in atomic level engineering of structure and properties. Here, the “surgery” refers to tailoring of specific sites in a cluster without changing the other parts (for example, just replacing specific surface motifs, and deleting one or two metal atoms). It helps decoding the roles of different parts of a nanocluster play in the properties.

Li et al. first reported the surface “surgery” of a 23-gold-atom $[Au_{23}(SR)_{16}]^-$ nanocluster by a two-step metal-exchange method.⁵⁰ The first-step was Ag-for-Au exchange, leading to the formation of a critical intermediate, $[Au_{23-x}Ag_x(SR)_{16}]^-$ ($x \sim 1$), which lowers the transformation barrier in the second step, i.e. the reaction with $Au_2Cl_2(P-C-P)$, where P-C-P stands for $Ph_2PCH_2PPh_2$. Overall, the “surgery” successfully replaced the S-Au-S staples with the P-C-P ones owing to their geometric resemblance, forming a new 21-gold-atom nanocluster of $[Au_{21}(SR)_{12}(P-C-P)_2]^+$ without changing the other parts of the original nanocluster (Figure 4). The optical absorption spectrum of $[Au_{21}(SR)_{12}(P-C-P)_2]^+$ is similar to that of $[Au_{23}(SR)_{16}]^-$ as well as $[Au_{23-x}Ag_x(SR)_{16}]^-$. Surprisingly, the photoluminescence (PL) efficiency of $[Au_{21}(SR)_{12}(P-C-P)_2]^+$ is found to be enhanced by ~ 10 times compared to that of $[Au_{23}(SR)_{16}]^-$. These results reveal that the surface motifs have little effects on the optical absorption but a distinct influence on the PL.

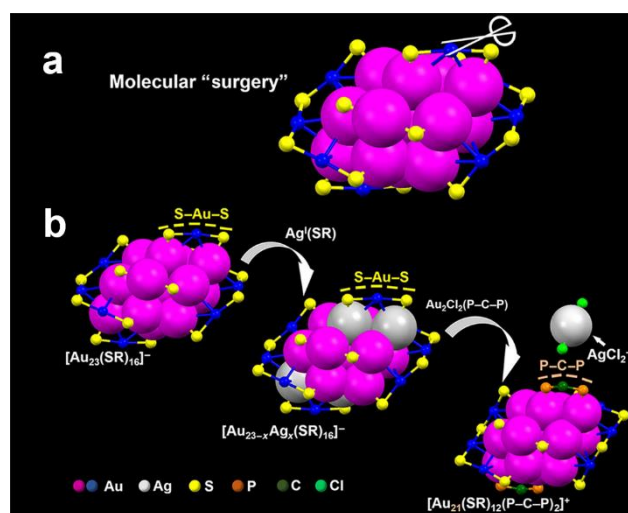


Figure 4. Molecular “surgery” on $[Au_{23}(SR)_{16}]^-$ by replacing the two organometallic RS-Au-SR surface motifs with two organic $Ph_2P-CH_2-PPh_2$ diphosphine ligands. Adapted with permission from ref. 50; Copyright © 2017, AAAS.

Surface-protecting ligand engineering

The surface-protecting ligands, as a major part of the nanocluster components, bring diversity to the nanoclusters.⁵¹ The alkynyl ligands ($RC\equiv C-$) form relatively strong interactions with coinage metals.⁵² Due to the dramatically different

bonding patterns (via both σ and π bonding) and large π -conjugated system, the alkynyl group brings unique surface motif geometry and modulates the electronic structures as reflected in optical absorption, luminescence and catalytic reactivity.⁵²

Interestingly, some of the alkynyl-protected gold nanoclusters $\text{Au}_{36}(\text{C}\equiv\text{CPh})_{24}$, $\text{Au}_{44}(\text{C}\equiv\text{CPh})_{28}$, $[\text{Au}_{38}(\text{C}\equiv\text{CPh})_{20}(\text{PPh}_3)_4]^{2+}$ and even the larger size $\text{Au}_{144}(\text{C}\equiv\text{CR})_{60}$ ⁵³⁻⁵⁵ could be viewed as the counterparts of thiolate protected $\text{Au}_{36}(\text{SR})_{24}$, $[\text{Au}_{38}(\text{SR})_{20}(\text{PPh}_3)_4]^{2+}$, $\text{Au}_{44}(\text{SR})_{28}$, and $\text{Au}_{144}(\text{SR})_{60}$.⁵⁶⁻⁵⁸ These pairs have almost identical gold core structures. Of note, the recently reported $\text{Au}_{22}(\text{C}\equiv\text{C}^t\text{Bu})_{18}$ has the similar structure as the theoretically proposed model of $\text{Au}_{22}(\text{SG})_{18}$,⁵⁹ (SG = thiolate of glutathione). Because these isostructural pairs differ only in the protecting ligands, they are ideal systems for studying the ligand effects on catalytic behavior. The alkynyl-protected $[\text{Au}_{38}(\text{C}\equiv\text{CPh})_{20}(\text{PPh}_3)_4]^{2+}$ was found to be more active in the semihydrogenation of alkynes to alkenes than the thiolated-capped $[\text{Au}_{38}(\text{SR})_{20}(\text{PPh}_3)_4]^{2+}$ (<2%) (Figure 5). This indicates the efficiency of ligand engineering in catalytic alkyne and H_2 activation reaction. The surface ligand may disturb the electronic structure, which accounts for the different catalytic performance. The surface ligand engineering has also been found in the mixed ligands (carboxylic acid and thiolate) protected Ag(I) cluster system, and the fluorescence, electrochemical activity and chirality of the Ag(I)₂₀ clusters can be modulated by functionalized carboxylic or amino acid substitution.⁶⁰

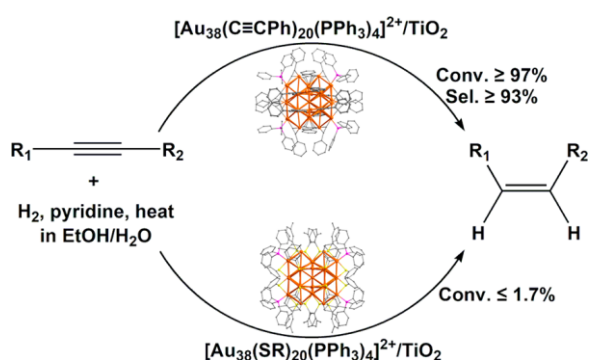


Figure 5. Catalytic performance of two supported Au_{38} nanoclusters for the semihydrogenation of alkynes. Adapted with permission from ref. 52; Copyright © 2018, American Chemical Society.

Charge state engineering

Magnetism is another intriguing and significant property for atomically precise nanoclusters.⁶¹⁻⁶³ It is known that single gold atoms are paramagnetic because of the unpaired $6s^1$ electron, while bulk gold is diamagnetic because the paramagnetism of the conduction electrons is counteracted by the orbital and ionic core diamagnetism. The nanocluster state lies in between atomic state and bulk metal, hence, it is critical to study the magnetism evolution.

The magnetic properties are closely related with the charge state of nanoclusters or the number of free valence electrons

in the core. It corresponds to the delocalized electrons that are responsible for the cluster stability and chemical reactivity. Two neutral, homogold nanoclusters have been reported to be magnetic, including $\text{Au}_{133}(\text{SR})_{52}$ (Figure 6a) and $\text{Au}_{25}(\text{SR})_{18}$ (Figure 6b). The most investigated case is the $\text{Au}_{25}(\text{SR})_{18}$, and controlling its charge state from -1 to 0 led to the transition from diamagnetism to paramagnetism (Figure 6b) probed by electron paramagnetic resonance (EPR) and nuclear magnetic resonance (NMR) measurements.^{63, 64} As shown in Figure 6c, paramagnetism of the neutral $[\text{Au}_{25}(\text{SR})_{18}]^0$ is due to the open shell electronic structure (i.e., 7 delocalized Au valence electrons distributed in the superatomic orbitals, $1S^21P^5$). The odd number of electron count leads to one unpaired electron. When the unpaired electron is removed by oxidation to $[\text{Au}_{25}(\text{SR})_{18}]^+$ (6e) or is paired with an electron via chemical reduction to $[\text{Au}_{25}(\text{SR})_{18}]^-$ (8e), the nanocluster becomes diamagnetic.

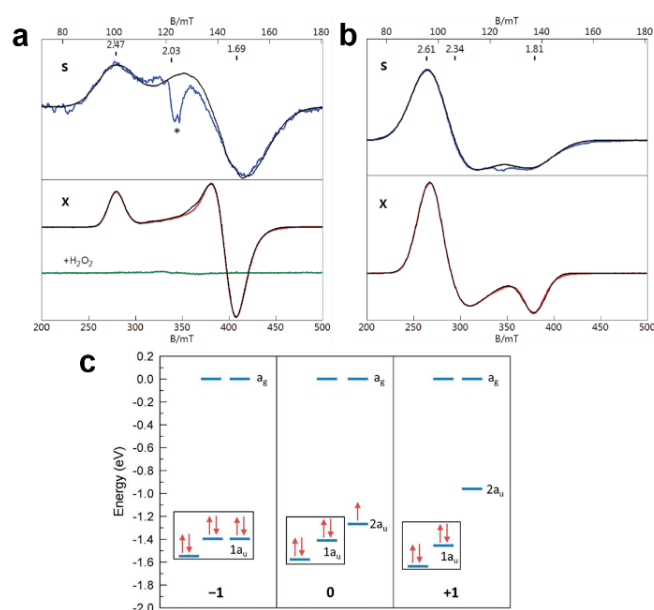


Figure 6. The S-band and X-band cryogenic EPR spectra of $[\text{Au}_{133}(\text{SR})_{52}]^0$ (a) and $[\text{Au}_{25}(\text{SR})_{18}]^0$ (b); note: the $g = 2.03$ signal (marked *) is from the extraneous copper. (c) Frontier orbital diagrams of $\text{Au}_{25}(\text{SCH}_3)_{18}^q$ ($q = -1, 0, +1$). Panels (a-b): adapted with permission from ref. 65; Copyright © 2019, Royal Society of Chemistry. Panel (c): adapted with permission from ref. 54; Copyright © 2013, American Chemical Society.

Similar charge state conversion has also been recently found in the $\text{Au}_{133}(\text{SR})_{52}$ nanocluster.⁶⁵ EPR analysis shows its paramagnetic character of axial symmetry with $g_x = g_y < g_z$ (Figure 6a), and the values are $g_{||} = 2.47$ and $g_{\perp} = 1.69$. The axial g -tensor for $\text{Au}_{133}(\text{SR})_{52}$ is in contrast to the non-axial $\text{Au}_{25}(\text{SR})_{18}$ with a g -tensor of (2.61, 2.34, 1.81) (Figure 6b). Quantification of $\text{Au}_{133}(\text{SR})_{52}$ signals shows that the neutral cluster possesses one unpaired electron. As $\text{Au}_{133}(\text{SR})_{52}$ has 81 nominal “valence electrons”, its paramagnetism (one spin per particle) also proves its nonmetallic electronic structure, because those electrons fill into discrete orbitals instead of a continuous band. Furthermore, oxidizing $[\text{Au}_{133}(\text{SR})_{52}]^0$ by H_2O_2

to $[\text{Au}_{133}(\text{SR})_{52}]^+$ removes the unpaired electron, thus, the nanocluster changes from paramagnetism to diamagnetism (Figure 6a, green line). The different magnetic moment symmetry between $\text{Au}_{133}(\text{SR})_{52}$ (axial g tensor) and $\text{Au}_{25}(\text{SR})_{18}$ (non-axial) indicates a change in symmetry of the orbital holding the spin, yet the similar range of delocalization of their spin wavefunctions is intriguing.⁶⁵ Future theoretical work may reveal more insight into the electronic structure of $\text{Au}_{133}(\text{SR})_{52}$.

Conclusion and outlook

Overall, the atomic level engineering of metal nanoclusters can be performed on the metal, ligand and charge state. As each component plays vital roles in maintaining the geometric and electronic structures of the nanoclusters, tailoring by single-atom alteration, ligand exchange, surface surgery, or single-electron control, may induce distinct changes to the physicochemical properties, manifested in the optical absorption, photoluminescence, catalytic activity, and magnetism. The electronic evolution from the discrete state to nascent plasmons^{66,67} is of particular interest and much remains to dig out in future work.

The atomic level engineering approaches hold promise in future development as versatile tools for tailoring and expanding the novel functionalities of nanoclusters. New applications are expected by precise control over the nanoclusters. For example, doping with ferromagnetic metals such as Fe, Co, and Ni, and incorporating rare earth elements for excellent photoluminescence performance. Therefore, more in-depth understanding of the atomic precision engineering is expected, it needs extensive investigation on larger size nanocluster systems, more variety of dopants, introduction of novel functional groups, and creative molecular "surgery" pathways.

Conflicts of interest

There are no conflicts to declare.

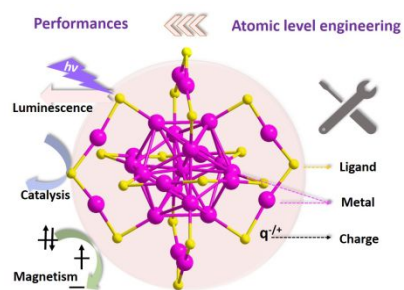
Acknowledgements

R.J. acknowledges financial support from the National Science Foundation (DMR-1808675).

Notes and references

- R. Jin, C. Zeng, M. Zhou and Y. Chen, *Chem. Rev.*, 2016, **116**, 10346-10413.
- N. A. Sakthivel and A. Dass, *Acc. Chem. Res.*, 2018, **51**, 1774-1783.
- I. Chakraborty and T. Pradeep, *Chem. Rev.*, 2017, **117**, 8208-8271.
- B. Bhattarai, Y. Zaker, A. Atmagulov, B. Yoon, U. Landman and T. P. Bigioni, *Acc. Chem. Res.*, 2018, **51**, 3104-3113.
- T. Higaki, Q. Li, M. Zhou, S. Zhao, Y. Li, S. Li and R. Jin, *Acc. Chem. Res.*, 2018, **51**, 2764-2773.
- X. Kang and M. Zhu, *Chem. Soc. Rev.*, 2019, **48**, 2422-2457.
- M. Zhou, T. Higaki, G. Hu, M. Y. Sfeir, Y. Chen, D. Jiang and R. Jin, *Science* 2019, **364**, 279-282.
- R. S. Dhayal, W. E. van Zyl and C. W. Liu, *Dalton Trans.*, 2019, **48**, 3531-3538.
- B. Nieto-Ortega and T. Bürgi, *Acc. Chem. Res.*, 2018, **51**, 2811-2819.
- M. Zhou, T. Higaki, Y. Li, C. Zeng, Q. Li, M. Y. Sfeir and R. Jin, *J. Am. Chem. Soc.*, 2019, **141**, 19754-19764.
- Z. Lei, X.-K. Wan, S.-F. Yuan, J.-Q. Wang and Q.-M. Wang, *Dalton Trans.*, 2017, **46**, 3427-3434.
- R. R. Nasaruddin, T. Chen, N. Yan and J. Xie, *Coord. Chem. Rev.*, 2018, **368**, 60-69.
- S. Kenzler, F. Fetzer, C. Schrenk, N. Pollard, A. R. Frojd, A. Z. Clayborne and A. Schnepf, *Angew. Chem. Int. Ed.* 2019, **58**, 5902-5905.
- Q. Yao, X. Yuan, T. Chen, D. T. Leong and J. Xie, *Adv. Mater.*, 2018, **30**, e1802751.
- A. Das, T. Li, K. Nobusada, C. Zeng, N. L. Rosi and R. Jin, *J. Am. Chem. Soc.*, 2013, **135**, 18264-18267.
- A. Das, T. Li, G. Li, K. Nobusada, C. Zeng, N. L. Rosi and R. Jin, *Nanoscale*, 2014, **6**, 6458-6462.
- M. Zhu, C. M. Aikens, F. J. Hollander, G. C. Schatz and R. Jin, *J. Am. Chem. Soc.*, 2008, **130**, 5883-5885.
- S. Zhao, A. Das, H. Zhang, R. Jin, Y. Song and R. Jin, *Prog. Nat. Sci.*, 2016, **26**, 483-486.
- A. Das, T. Li, K. Nobusada, Q. Zeng, N. L. Rosi and R. Jin, *J. Am. Chem. Soc.*, 2012, **134**, 20286-20289.
- S. Wang, H. Abroshan, C. Liu, T.-Y. Luo, M. Zhu, H. J. Kim, N. L. Rosi and R. Jin, *Nat. Commun.*, 2017, **8**, 848.
- X. Cai, W. Hu, S. Xu, D. Yang, M. Chen, M. Shu, R. Si, W. Ding and Y. Zhu, *J. Am. Chem. Soc.*, 2020, **142**, 4141-4153.
- Z. Gan, N. Xia and Z. Wu, *Acc. Chem. Res.*, 2018, **51**, 2774-2783.
- S. Hossain, Y. Niihori, L. V. Nair, B. Kumar, W. Kurashige and Y. Negishi, *Acc. Chem. Res.*, 2018, **51**, 3114-3124.
- A. Ghosh, O. F. Mohammed and O. M. Bakr, *Acc. Chem. Res.*, 2018, **51**, 3094-3103.
- S. Wang, Q. Li, X. Kang and M. Zhu, *Acc. Chem. Res.*, 2018, **51**, 2784-2792.
- X. Du, J. Chai, S. Yang, Y. Li, T. Higaki, S. Li and R. Jin, *Nanoscale* 2019, **11**, 19158-19165.
- X. Kang, X. Wei, S. Jin, Q. Yuan, X. Luan, Y. Pei, S. Wang, M. Zhu, and R. Jin, *Proc. Natl. Acad. Sci. USA*, 2019, **116**, 18834-18840.
- S. Wang, Y. Song, S. Jin, X. Liu, J. Zhang, Y. Pei, X. Meng, M. Chen, P. Li and M. Zhu, *J. Am. Chem. Soc.*, 2015, **137**, 4018-4021.
- S. L. Christensen, M. A. MacDonald, A. Chatt, P. Zhang, H. Qian and R. Jin, *J. Phys. Chem. C*, 2012, **116**, 26932-26937.
- Y. Negishi, K. Munakata, W. Ohgake and K. Nobusada, *J. Phys. Chem. Lett.*, 2012, **3**, 2209-2214.
- S. Xie, H. Tsunoyama, W. Kurashige, Y. Negishi and T. Tsukuda, *ACS Catal.*, 2012, **2**, 1519-1523.
- M. Zhou, C. Yao, M. Y. Sfeir, T. Higaki, Z. Wu and R. Jin, *J. Phys. Chem. C*, 2018, **122**, 13435-13442.
- K. Kwak, Q. Tang, M. Kim, D.-e. Jiang and D. Lee, *J. Am. Chem. Soc.*, 2015, **137**, 10833-10840.
- Y. Negishi, W. Kurashige, Y. Niihori, T. Iwasa and K. Nobusada, *Phys. Chem. Chem. Phys.*, 2010, **12**, 6219-6225.
- W. Fei, S. Antonello, T. Dainese, A. Dolmella, M. Lahtinen, K. Rissanen, A. Venzo and F. Maran, *J. Am. Chem. Soc.*, 2019, **141**, 16033-16045.
- C. Yao, Y.-J. Lin, J. Yuan, L. Liao, M. Zhu, L.-H. Weng, J. Yang and Z. Wu, *J. Am. Chem. Soc.*, 2015, **137**, 15350-15353.
- L. Liao, S. Zhou, Y. Dai, L. Liu, C. Yao, C. Fu, J. Yang and Z. Wu, *J. Am. Chem. Soc.*, 2015, **137**, 9511-9514.

38. D. R. Kauffman, D. Alfonso, C. Matranga, H. Qian and R. Jin, *J. Phys. Chem. C*, 2013, **117**, 7914-7923.
39. C. Kumara, C. M. Aikens and A. Dass, *J. Phys. Chem. Lett.*, 2014, **5**, 461-466.
40. M. S. Bootharaju, C. P. Joshi, M. R. Parida, O. F. Mohammed and O. M. Bakr, *Angew. Chem. Int. Ed.*, 2016, **55**, 922-926.
41. X. Liu, J. Yuan, C. Yao, J. Chen, L. Li, X. Bao, J. Yang and Z. Wu, *J. Phys. Chem. C*, 2017, **121**, 13848-13853.
42. J. Yan, H. Su, H. Yang, S. Malola, S. Lin, H. Häkkinen and N. Zheng, *J. Am. Chem. Soc.*, 2015, **137**, 11880-11883.
43. Y. Li, T.-Y. Luo, M. Zhou, Y. Song, N. L. Rosi and R. Jin, *J. Am. Chem. Soc.*, 2018, **140**, 14235-14243.
44. X. Kang, M. Zhou, S. Wang, S. Jin, G. Sun, M. Zhu and R. Jin, *Chem. Sci.*, 2017, **8**, 2581-2587.
45. R. Juarez-Mosqueda, S. Malola and H. Häkkinen, *Phys. Chem. Chem. Phys.*, 2017, **19**, 13868-13874.
46. A. Chen, X. Kang, S. Jin, W. Du, S. Wang and M. Zhu, *J. Phys. Chem. Lett.*, 2019, **10**, 6124-6128.
47. a) S. K. Barik, T.-H. Chiu, Y.-C. Liu, M.-H. Chiang, F. Gam, I. Chantrenne, S. Kahlal, J.-Y. Saillard and C. W. Liu, *Nanoscale*, 2019, **11**, 14581-14586; b) T.-H. Chiu, J.-H. Liao, F. Gam, I. Chantrenne, S. Kahlal, J.-Y. Saillard and C. W. Liu, *J. Am. Chem. Soc.* 2019, **141**, 12957-12961; c) W.-T. Chang, P.-Y. Lee, J.-H. Liao, S. Kahlal, K. K. Chakrahari, J.-Y. Saillard and C. W. Liu, *Angew. Chem. Int. Ed.* 2017, **56**, 10178-10182.
48. X.-J. Xi, J.-S. Yang, J.-Y. Wang, X.-Y. Dong and S.-Q. Zang, *Nanoscale*, 2018, **10**, 21013-21018.
49. Y. Liu, X. Chai, X. Cai, M. Chen, R. Jin, W. Ding and Y. Zhu, *Angew. Chem. Int. Ed.*, 2018, **57**, 9775-9779.
50. Q. Li, T.-Y. Luo, M. G. Taylor, S. Wang, X. Zhu, Y. Song, G. Mpourmpakis, N. L. Rosi and R. Jin, *Sci. Adv.*, 2017, **3**, e1603193.
51. A. Tlahuice-Flores, *Phys. Chem. Chem. Phys.*, 2016, **18**, 27738-27744.
52. Z. Lei, X.-K. Wan, S.-F. Yuan, Z.-J. Guan and Q.-M. Wang, *Acc. Chem. Res.*, 2018, **51**, 2465-2474.
53. X.-K. Wan, Z.-J. Guan and Q.-M. Wang, *Angew. Chem. Int. Ed.*, 2017, **56**, 11494-11497.
54. X.-K. Wan, J.-Q. Wang, Z.-A. Nan and Q.-M. Wang, *Sci. Adv.*, 2017, **3**, e1701823.
55. Z. Lei, J.-J. Li, X.-K. Wan, W.-H. Zhang and Q.-M. Wang, *Angew. Chem. Int. Ed.*, 2018, **57**, 8639-8643.
56. C. Zeng, H. Qian, T. Li, G. Li, N. L. Rosi, B. Yoon, R. N. Barnett, R. L. Whetten, U. Landman and R. Jin, *Angew. Chem. Int. Ed.*, 2012, **51**, 13114-13118.
57. C. Zeng, Y. Chen, K. Iida, K. Nobusada, K. Kirschbaum, K. J. Lambright and R. Jin, *J. Am. Chem. Soc.*, 2016, **138**, 3950-3953.
58. N. Yan, N. Xia, L. Liao, M. Zhu, F. Jin, R. Jin and Z. Wu, *Sci. Adv.*, 2018, **4**, eaat7259.
59. Y. Pei, J. Tang, X. Tang, Y. Huang and X. C. Zeng, *J. Phys. Chem. Lett.*, 2015, **6**, 1390-1395.
60. S. Li, X. Du, B. Li, J.-Y. Wang, G.-P. Li, G.-G. Gao and S.-Q. Zang, *J. Am. Chem. Soc.*, 2018, **140**, 594-597.
61. M. Agrachev, M. Ruzzi, A. Venzo and F. Maran, *Acc. Chem. Res.*, 2019, **52**, 44-52.
62. S. Tian, L. Liao, J. Yuan, C. Yao, J. Chen, J. Yang and Z. Wu, *Chem. Commun.*, 2016, **52**, 9873-9876.
63. M. Zhu, C. M. Aikens, M. P. Hendrich, R. Gupta, H. Qian, G. C. Schatz and R. Jin, *J. Am. Chem. Soc.*, 2009, **131**, 2490-2492.
64. S. Antonello, N. V. Perera, M. Ruzzi, J. A. Gascón and Flavio Maran, *J. Am. Chem. Soc.*, 2013, **135**, 15585-15594.
65. C. Zeng, A. Weitz, G. Withers, T. Higaki, S. Zhao, Y. Chen, R. R. Gil, M. Hendrich and R. Jin, *Chem. Sci.*, 2019, **10**, 9684-9691.
66. T. Higaki, M. Zhou, K. J. Lambright, K. Kirschbaum, M. Y. Sfeir and R. Jin, *J. Am. Chem. Soc.* 2018, **140**, 5691-5695.
67. T. Higaki, M. Zhou, G. He, S. D. House, M. Y. Sfeir, J. C. Yang and R. Jin, *Proc. Natl. Acad. Sci. USA* 2019, **116**, 13215-13220.



This frontier article illustrates single-atom, single-electron level engineering for tailoring the properties of metal nanoclusters using gold as a model.